Submitted for publication in ICNS Proceedings

Towards 0.1 mm spatial resolution

A. D. Stoica and X. L. Wang*

Spallation Neutron Source

701 Scarboro Road

Oak Ridge National Laboratory

Oak Ridge, TN 37831, USA

Abstract

A design goal for VULCAN, the SNS engineering diffractometer, is to enable spatial mapping with 0.1 mm resolution. Because the targeted applications often involve the use of large samples or special environment, slits cannot be used for this purpose. In this paper, methods to achieve 0.1 mm spatial resolution are outlined. For the incident beam, a new compact focusing device is proposed. The device is made of a stack of bent silicon wafers, each having a reflective multilayer (supermirror) deposited on one side and a neutron-absorbing layer on the other side. The optimal design to minimize the optical spatial aberrations is discussed and Monte-Carlo simulation results are presented. For the diffracted beam, imaging devices made from thick packets of diffracting bent silicon wafers (known as the Bragg Mirrors) could be used. The requirements to achieve a sharp imaging together with a large phase-space acceptance window are discussed and preliminary testing results are presented.

PACS: 61.12.Ex

* Corresponding author. (Fax: +001/865-241-5177, E-mail: wangxl@ornl.gov)

One of the challenging tasks of neutron diffraction in engineering applications is to achieve submillimeter spatial resolution [1]. This is not only related with the mapping of phase content, residual strain and/or texture in fine grained polycrystalline materials, but also with the possibility of performing grain by grain measurements in coarse grained materials. The best spatial resolution of existing engineering diffractometers is around 1 mm^3 obtained by using the pinhole technique (slits before and after scattering). Due to the large dimensions of the investigated samples in most engineering measurements, the distance from slit to the sampling volume can be quite large (e.g., ~ 300 mm). Then the reduction of the sampling volume demands not only the reduction of the slit dimensions but also a reduction of the beam angular divergence far below the value necessary for a good angular resolution in diffraction. In these conditions the use of pinhole technique involves a dramatic decrease in intensity to enhance the spatial resolution.

It is thus clear that for mapping experiments with high spatial resolution, the use of focusing techniques is essential. From this point of view the first problem would be to find a method to deliver a sharp spatially shaped neutron beam to the sample with the goal to probe thin slices of sample. Secondly, we need a method to obtain an image of the illuminated area of the sample in the 'light' of diffracted neutrons using position sensitive detectors (PSD). The following discussion concentrates on two new ideas of imaging devices able to be used in time of flight diffractometry for solving these two problems.

1. Focusing multi-channel

Polycapillary optics has shown exciting capabilities to focus neutrons at a submillimeter scale [2]. However the devices designed on this principle have a modest transmission (less than 10%). The reported flux gains are basically given by the high angular divergence at focus (usually > 10 degrees).

Moreover, the focusing distance is small (a few millimeters only). These two features drastically limit the possibility of using polycapillary optics in neutron scattering where angular divergences are limited and distance to the sample is an important parameter.

Another way to design compact focusing devices comes from the Soller collimator concept. Stacks of silicon wafers (straight or curved) coated with reflective and/or absorbing surfaces can be used as collimators [3-4], benders [5], multiple reflections focusing micro-guides [6], or single reflection focusing devices [7].

The proposed optical device, here below referred to as the focusing multi-channel or FMC, consists from a stack of silicon wafers having a reflective multilayer (supermirror) deposited on one side of each wafer and an absorbent layer on the other side (Fig.1a), covering the reflective multilayer of the neighboring wafer. All wafers are curved in the horizontal plane at a fixed radius of curvature (R_0) with the multilayer on the convex side of the wafer. Each multilayer will reflect neutrons as a cylindrical concave mirror in a limited angular range determined by the multilayer length and by the distance from the source (considered here a point source placed in the focal plane) to the multilayer. The line of sight is defined as the straight line connecting the focal points of the device, f being the *focal length of the device*. The device is placed out of the line of sight (Fig.1b). The wafer *thickness* g_0, the *height* H_0 and the *length* L_0 are constant, but the *length of the deposition* L_n is variable, where n represents the reflecting multilayer number.

The device design was optimized by an iterative procedure to achieve a minimal spatial aberration in the image focal plane with the source placed at focus. Using this procedure the following constructive data were obtained: f = 3 m, R_0 = 580 m, L_0 = 60 mm and g_0 = 0.2 mm. The minimal angle accepted by the device (relative to the beam axis direction) is almost 0.2°. Each channel reflects neutrons in an

average angular range of 0.004°. An overall acceptance of 0.3° is obtained for 80 wafers with an overall thickness of 16 mm. This angular divergence of the beam is considered appropriate for the time-of-flight diffraction requirements.

The spatial beam profile was calculated by Monte Carlo method for different locations of a point source across the beam direction in the focal plane. While the intensity profile is almost triangular for a point source located on the opposite side of the multi-channel device, long tails appear when the point source is on the same side of the multi-channel with a sharper peak. In all cases, the FWHM of spatial distribution is less than 0.1 mm.

The geometrical transmission of multi-channel device can be considered unity if the point source is placed at the focus point. The transmission decreases when the point source is displaced from the focal point, becoming about 50% when the displacement is ± 8 mm. To account for the reflection losses, a supermirror with M = 3.5 was considered. Introducing the reflectivity profile and the beam attenuation through silicon, the actual transmission for a point source at the focus was estimated to be 80% for 1.5-4.5 Å neutrons. Below 1.4 Å, the transmission gradually decreases to 40%, because the overall angular acceptance is limited by the critical angle of supermirror.

2. Bragg mirrors

Theoretical examination of neutron imaging by Bragg reflection from bent crystals was undertaken recently [8]. A result that came as a surprise was that thick multi-wafer packets could provide sharp imaging even if the incident beam has a broad distribution of wavelengths. The image blurring is canceled when two conditions of non-dispersive (i.e., independent of wavelength) imaging are met. With thick packets of silicon wafers the spatial resolution of the non-dispersive image is limited by the thickness of

a single wafer rather than by the overall thickness of the packet. Such devices have been called Bragg mirrors (BM) [9].

To use the BM non-dispersive imaging properties, the distances to the object, L_0, and to the image, L_1, should be set at some characteristic values given by, $L_0 = (R_H/2)\sin(2q)\ \mathrm{sgn}(q+c)/\cos(q-c)$ and $L_1 = (R_H/2)\sin(2q)\ \mathrm{sgn}(q+c)/\cos(q+c)$. Here, R_H is the horizontal curvature radius, $2q$ the Bragg angle, c the cutting angle of the crystal. The magnification of the BM given by the distance ratio becomes: $M = \cos(q-c)/\cos(q+c)$. Note that only when $M > 0$ is the image real, which may be recorded with a PSD.

A mirror is *astigmatic* if the image positions in the equatorial (horizontal) and sagittal (vertical) planes are different. The astigmatism of the BM is canceled *(stigmatic imaging)* when the lens focusing relation in the vertical plane is also fulfilled. This leads to a connection between the sagittal curvature radius, R_V, and the equatorial curvature radius, R_H: $R_V = R_H\ \mathrm{sgn}(q+c)\sin^2 q$. To avoid exceeding the elastic limit of the crystal, the sagittal curvature can be realized by segmentation.

The spatial resolution of the image is determined by the optical quality of the BM and by the spatial resolution of the PSD, as the image blurring due to the intrinsic diffraction range in a perfect crystal is usually negligible (less that 5 μm at $R_H \sim 1$ m). For curved multi-wafer packets, the main aberration term comes from the elastic deformation of the wafers. A tangential stress gradient is generated inside the crystal on curving. This gradient not only changes the *d*-spacing, but also rotates the crystalline planes if they are not parallel to the crystal surface. The aberration term due to wafer deformation is proportional to *sinc* and to the wafer thickness. Consequently this term vanishes when $c=0$. Otherwise it can be minimized with thinner wafers that are available commercially down to 10 μm. Additional blurring may

occur due to imperfections of the device (wafer misalignment, non-uniformity of the thickness and of the horizontal radius). The practical limit of spatial resolution is expected to be around 100 μm.

Experimental test made at Missouri University Research Reactor (MURR) proved some basic features of BM arrangements with multi-wafers [10]. The ultimate imaging resolution possible with a BM configuration can be seen in measurements using a single wafer. As an example the results obtained with a Si[111] wafer on (220) reflection are presented in Fig. 3. The object was a cadmium plate with three slits of 0.5 mm wide and 3 mm apart. The image was brought to the computed position by varying the analyzer curvature. It was scanned with a narrow (0.2 mm) slit. To simulate the white beam associated with a TOF arrangement the incident neutron wavelength was varied. Because of the limited beam angular divergence (less than 1°), a full mapping of the phase space acceptance window could not be achieved.

In Fig. 3, the detector angular position was converted into the coordinate across the object and the monochromator angle was converted into the relative variation of wavelength. The FWHM of the image (for 0.5 mm wide slits) is only 0.54 mm, indicating very little smearing. Moreover, the positions of the image do not depend on the wavelength. Fig. 3 also illustrates that despite the limited incident beam divergence, the BM accepts a bandwidth of no less than 2% ($\Delta\lambda/\lambda$), sufficient to capture a diffraction peak from even heavily deformed samples.

A magnifying configuration (M = 2.8) was chosen to minimize the wafer thickness contribution and the PSD smearing in a real design. By considering the standard deviation of the peak profile and subtracting the contributions of the object slit and the receiving slit, one gets a spatial resolution of less than 0.28 mm FWHM in the Gaussian approximation with a 70 μm thick wafer in the BM configuration. Spatial resolutions down to 0.1 mm should be obtainable by reducing the wafer thickness by a factor of

2-3. A high-quality wafer surface is required to achieve such resolution, since tests using an unpolished wafer have demonstrated a dramatic smearing of the image.

On a pulse neutron source, a BM together with a PSD allows simultaneous mapping in both real space and scattering space. This type of device could be used for a TOF engineering diffractometer like VULCAN in order to achieve 0.1 mm spatial resolution in the diffracted neutron beam. Analysis by numerical methods indicate that at $2q_S = 90^0$ (the most attractive case for imaging in scattering), the lattice spacing resolutions better than 0.5% can be achieved with a relative acceptance window of $\Delta\lambda/\lambda$ greater than 6%. For a given $\Delta\lambda/\lambda$, the resolution further improves at higher scattering angles. In any case, with a BM, it should be possible to record a single diffraction peak or a few close peaks along with their higher orders.

3. Conclusions

The proposed focusing multi-channel device, designed to deliver spatially shaped neutron beams with one-dimensional 0.1 mm resolution over a large range of neutron wavelengths, shows promising capabilities for time-of-flight diffraction. To achieve the performances predicted by the present estimations, hard technical requirements should be fulfilled concerning the mirror quality, wafer assembling accuracy and curvature radius control. These issues are subject of future experimental testing.

The Bragg mirror with curved silicon multi-wafers can provide sharp imaging in white neutron beams. Preliminary tests have demonstrated the capability of neutron imaging with BM at a spatial resolution of 0.3 mm and magnifications of about 3. To push the spatial resolution close to 0.1 mm, further development of silicon multi-wafer devices is needed. Estimations show that with BM imaging,

the data rate in spatial mapping can be increased by an order of magnitude when compared with the sequential pinhole probing method.

References:

[1] X.-L. Wang, "Conceptual Design of the SNS Engineering Diffractometer", SNS Report No. IS-1.1.8.2-6035-RE-A-00; T. M. Holden, "Science Case for the VULCAN Diffractometer", SNS Report No. IS-1.7.9-6055-RE-A-00, both available at http://www.sns.anl.gov/ScatInst/Instrument/EnDi.htm

[2] H. H. Chen-Mayer, D. F. R. Mildner, V. A. Sharov, Q. F. Xiao, Y. T. Cheng, R. M. Lindstrom, and R. L. Paul, *Rev. Sci. Instrum.* **68**, 3744-3750 (1997).

[3] Th. Krist and F. Mezei, *Nucl. Instrum. Meth.* **A450**, 389-390 (2000).

[4] L. D. Cussen,P. Hoghoj, and I. S. Anderson, *Nucl. Instrum. Meth.* **A460**, 374-380 (2001).

[5] Th. Krist and F. Mezei, *Physica* **B 276-78**, 208-209 (1998).

[6] U. Gruning, A. Magerl, and D. F. R. Mildner, *Nucl. Instrum. Meth.* **A314**, 171-177 (1992).

[7] M. W. Johnson and M. R. Daymond, *Physica* **B 283**, 308-313(2000).

[8] A. D. Stoica, M. Popovici, C. R. Hubbard: J. Appl. Cryst. **34**, 343 (2001).

[9] A. D. Stoica, M. Popovici, C. R. Hubbard, *ORNL / TM2000 /* **207**, 2000.

[10] M. Popovici, A. D. Stoica: this conference.

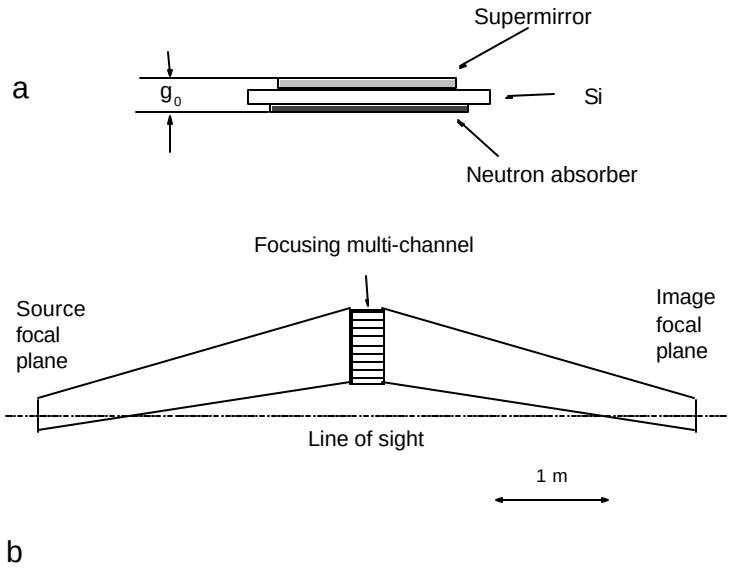

Fig. 1: Schematic diagram for: a) single wafer; b) multi-channel arrangement (vertical scale is highly exaggerated).

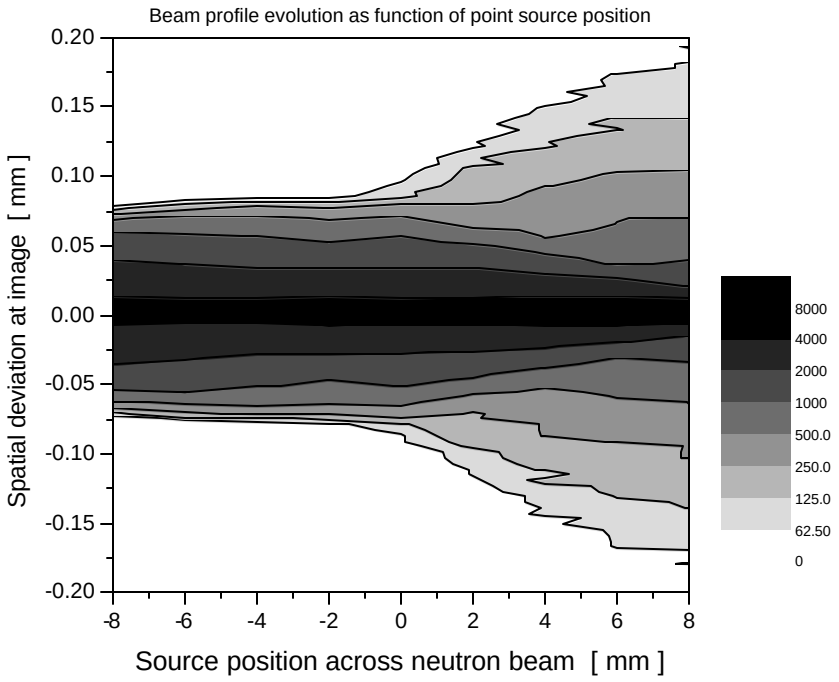

Fig. 2: Intensity distribution map as function of source position and spatial deviation at image. Note that the level of shade is in log scale in order to illustrate the appearance of long tails.

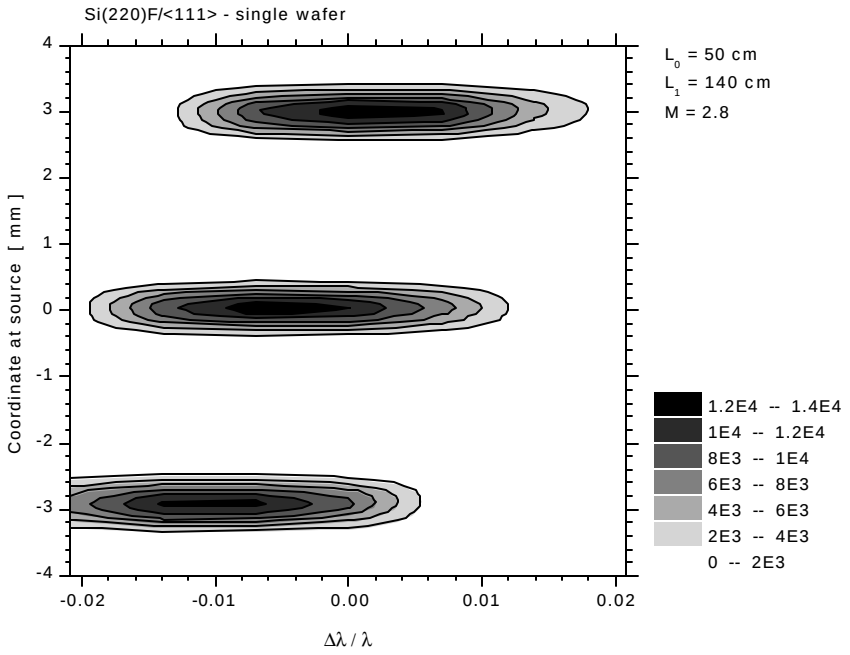

Fig. 3: Neutron imaging with one wafer (M = 2.8) – scan as function of incident neutron wavelength (in relative units) and detector slit position (converted into object coordinate).